



THE UNIVERSITY OF TOKYO

Research Center for the Early Universe

RESCEU-29/97

UTAP-266/97

## Cosmological Implications of Number Counts of Clusters of Galaxies: log $N$ –log $S$ in X-Ray and Submm Bands

Tetsu KITAYAMA,<sup>1</sup> Shin SASAKI,<sup>2</sup> and Yasushi SUTO<sup>1,3</sup>

<sup>1</sup> *Department of Physics, The University of Tokyo, Tokyo 113*

*E-mail(TK): kitayama@utaphp2.phys.s.u-tokyo.ac.jp*

<sup>2</sup> *Department of Physics, Tokyo Metropolitan University, Hachioji, Tokyo 192-03*

<sup>3</sup> *Research Center for the Early Universe, School of Science, The University of Tokyo, Tokyo 113*

### ABSTRACT

We compute the number counts of clusters of galaxies, the log $N$ –log $S$  relation, in several X-ray and submm bands on the basis of the Press-Schechter theory. We pay particular attention to a set of theoretical models which well reproduce the *ROSAT* 0.5–2 keV band log $N$ –log $S$ , and explore possibilities to further constrain the models from future observations with *ASCA* and/or at submm bands. The latter is closely related to the European *PLANCK* mission and the Japanese Large Millimeter and Submillimeter Array (*LMSA*) project. We exhibit that one can break the degeneracy in an acceptable parameter region on the  $\Omega_0 - \sigma_8$  plane by combining the *ROSAT* log $N$ –log $S$  and the submm number counts. Models which reproduce the *ROSAT* band log $N$ –log $S$  will have  $N(> S) \sim (150 - 300)(S/10^{-12} \text{ erg cm}^{-2} \text{ s}^{-1})^{-1.3} \text{ str}^{-1}$  at  $S \gtrsim 10^{-12} \text{ erg cm}^{-2} \text{ s}^{-1}$  in the *ASCA* 2–10 keV band, and  $N(> S_\nu) \sim (10^2 - 10^4)(S_\nu/100 \text{ mJy})^{-1.5} \text{ str}^{-1}$  at  $S_\nu \gtrsim 100 \text{ mJy}$  in the submm band ( $\lambda = 0.85 \text{ mm}$ ). The amplitude of the log $N$ –log $S$  is very sensitive to the model parameters in the submm band. We also compute the redshift evolution of the cluster number counts and compare with that of the X-ray brightest Abell-type clusters. The results, although still preliminary, point to low density ( $\Omega_0 \sim 0.3$ ) universes. The contribution of clusters to the X-ray and submm background radiations is shown to be at most 20% in any model compatible with the *ROSAT* log $N$ –log $S$ .

*Subject headings:* Cosmology — Galaxies : clusters of — Radio sources : extended — X-rays : sources

*submitted to Publications of the Astronomical Society of Japan*

## 1. Introduction

Clusters of galaxies are among the largest virialized structures in the universe and their importance as a cosmological probe is well-recognized. Thus their observations have been actively carried out in a variety of wavelengths including X-ray, optical, infrared, and radio bands. In the present paper, we focus on the theoretical predictions for the number counts of clusters of galaxies, the  $\log N$ – $\log S$  relation, rather than more conventional statistics such as the X-ray temperature and luminosity functions (hereafter XTF and XLF) for several reasons; 1) temperature of X-ray clusters can be reliably determined only for luminous ones, and thus the statistics is inevitably limited, 2) such obtained XTF is to some extent weighted towards relatively rich clusters, and may be biased for the luminous species, 3) the XTF and XLF at high redshifts ( $z \gtrsim 0.1$ ) are in fact model-dependent statistics, because the translation of the observed X-ray flux to the absolute luminosity, and of the observed number to the comoving number density can be done only by assuming specific values of the cosmological parameters (the density parameter,  $\Omega_0$ , the dimensionless cosmological constant,  $\lambda_0$ , and the Hubble constant  $H_0$  in units of 100 km/s/Mpc,  $h$ ).

On the other hand, the  $\log N$ – $\log S$  relation is free from the above problems as long as the cluster identification (or separation from point-like sources) is reliable. Recent analysis of the *ROSAT* Deep Cluster Survey (RDCS, Rosati et al. 1995, 1997) and the *ROSAT* Brightest Cluster Sample (BCS, Ebeling et al. 1997a,b) has determined the  $\log N$ – $\log S$  of clusters over almost four orders of magnitude in flux, i.e.  $S(0.5\text{--}2.0 \text{ keV}) \sim 10^{-14} - 10^{-10} \text{ erg cm}^{-2} \text{ s}^{-1}$ . The number of identified clusters in the  $\log N$ – $\log S$  is over 200, an order of magnitude larger than that for the commonly used XTF based on Henry & Arnaud (1991), and therefore the  $\log N$ – $\log S$  data are statistically more reliable.

Kitayama & Suto (1997, hereafter KS97) found that a set of cold dark matter (CDM) models reproduce the above *ROSAT*  $\log N$ – $\log S$  data remarkably well over whole observed flux range, and simultaneously agree with the observed XTF and the *COBE* 4 year data. Nevertheless, there still exist some degeneracy of acceptable parameters, for both cosmology and the intracluster gas properties. In the present paper, we explore possibilities to further constrain the models so as to break such degeneracy and discuss their implications in the following manner.

First, we combine the  $\log N$ – $\log S$  relations at different wavelengths, in X-ray and submm bands. The latter is of particular significance in relation to the future projects including the European *PLANCK* mission and the Japanese Large Millimeter and Submillimeter Array (*LMSA*) project. The emissions from intracluster gas in X-ray and submm bands are originated from completely different physical mechanisms; the former is mainly due to thermal bremsstrahlung, and the latter is due to the inverse-Compton scattering of the cosmic microwave background (CMB) photons, i.e. the Sunyaev & Zel'dovich (1972, hereafter SZ) effect. As a result, the  $\log N$ – $\log S$  relations in these bands show very different parameter dependence. We note that the submm  $\log N$ – $\log S$  was computed earlier by several authors (e.g., Barbosa et al. 1996;

Colafrancesco et al. 1997). Our analysis below differs from theirs in considering several CDM models consistent with the *ROSAT*  $\log N$ – $\log S$  data, in including the relativistic correction to the SZ effect, and in making quantitative and extensive predictions for the number counts on the  $\Omega_0 - \sigma_8$  plane.

Secondly, we consider the cluster number counts incorporating redshift and/or temperature information in addition to the flux. In this way, we are able to discuss the evolution of cluster abundances on the basis of a cosmological model-independent and bias-free observable at high redshifts, which is in contrast to the approaches based on the XTF or XLF. We demonstrate a tentative comparison of our predictions with an observed sample from the *ROSAT* All Sky Survey, the X-ray brightest Abell-type clusters (Ebeling et al. 1996).

Finally, we discuss the implications of our results for the X-ray background (XRB) and the submm background radiation (SBR). Since the  $\log N$ – $\log S$  relation is closely related to the background radiation in the corresponding energy band, we may rigorously constrain the contribution of clusters of galaxies to the XRB and SBR.

## 2. Number counts of clusters of galaxies in X-ray and submm bands

### 2.1. X-ray flux from clusters

Following KS97, we compute the number of clusters observed per unit solid angle with X-ray flux greater than  $S$  by

$$N(> S) = \int_0^\infty dz \, d_A^2(z) c \left| \frac{dt}{dz} \right| \times \int_S^\infty dS \, (1+z)^3 n_M(M, z) \frac{dM}{dT_{\text{gas}}} \frac{dT_{\text{gas}}}{dL_{\text{band}}} \frac{dL_{\text{band}}}{dS}, \quad (1)$$

where  $c$  is the speed of light,  $t$  is the cosmic time,  $T_{\text{gas}}$  and  $L_{\text{band}}$  are respectively the gas temperature and the band-limited absolute luminosity of clusters, and  $n_M(M, z)dM$  is the comoving number density of virialized clusters of mass  $M \sim M + dM$  at redshift  $z$ . If we write the angular diameter distance,  $d_A(z)$  as  $(c/H_0)D_A(z)$ , the dimensionless quantity  $D_A(z)$  is explicitly given by

$$D_A(z) = \frac{1}{1+z} \begin{cases} \sin(\sqrt{K}\chi)/\sqrt{K} & (K > 0) \\ \chi & (K = 0) \\ \sinh(\sqrt{-K}\chi)/\sqrt{-K} & (K < 0) \end{cases}, \quad (2)$$

where  $K = \Omega_0 + \lambda_0 - 1$ , and the radial distance  $\chi(z)$  is

$$\chi(z) = \int_0^z \frac{dz}{\sqrt{\Omega_0(1+z)^3 - K(1+z)^2 + \lambda_0}}. \quad (3)$$

Given the observed flux  $S$  in an X-ray energy band  $[E_a, E_b]$ , the source luminosity  $L_{\text{band}}$  at  $z$  in the corresponding band  $[E_a(1+z), E_b(1+z)]$  is written as

$$L_{\text{band}}[E_a(1+z), E_b(1+z)] = 4\pi d_L^2(z) S[E_a, E_b], \quad (4)$$

where  $d_L = (1+z)^2 d_A$  is the luminosity distance. Since the X-ray luminosity of clusters of galaxies depends sensitively on the details of the cluster gas density properties (distribution and clumpiness), its theoretical prediction as a function of  $M$  or  $T_{\text{gas}}$  is difficult. In fact, a simple self-similar model predicts for the bolometric luminosity,  $L_{\text{bol}} \propto T_{\text{gas}}^2$ , which is inconsistent with the observed relation  $L_{\text{bol}} \propto T_{\text{gas}}^{3 \sim 3.5}$ . Although a preheated cluster model might account for the latter (Kaiser 1991; Evrard & Henry 1991; Bower 1997), such theoretical models have not yet been specified. Thus we adopt the observed  $L_{\text{bol}} - T_{\text{gas}}$  relation parameterized by

$$L_{\text{bol}} = L_{44} \left( \frac{T_{\text{gas}}}{6 \text{keV}} \right)^\alpha (1+z)^\zeta 10^{44} h^{-2} \text{ erg sec}^{-1}. \quad (5)$$

As in KS97, we take  $L_{44} = 2.9$ ,  $\alpha = 3.4$  and  $\zeta = 0$  as a fiducial set of parameters on the basis of recent observational indications (David et al. 1993; Ebeling et al. 1996; Ponman et al. 1996; Mushotzky & Scharf 1997). Then we translate  $L_{\text{bol}}(T_{\text{gas}})$  into the band-limited luminosity  $L_{\text{band}}[T_{\text{gas}}, E_1, E_2]$  as

$$\begin{aligned} L_{\text{band}}[T_{\text{gas}}, E_a(1+z), E_b(1+z)] \\ = L_{\text{bol}}(T_{\text{gas}}) \times f[T_{\text{gas}}, E_a(1+z), E_b(1+z)], \end{aligned} \quad (6)$$

where  $f[T_{\text{gas}}, E_1, E_2]$  is the band correction factor which takes account of metal line emissions (Masai 1984) in addition to the thermal bremsstrahlung; the former makes significant contribution to the soft band luminosity especially at low temperature. Throughout this paper, we fix the abundance of intracluster gas as 0.3 times the solar value. Equations (4), (5) and (6) relate  $S$  and  $T_{\text{gas}}$  through  $L_{\text{band}}$ , and are used to compute equation (1).

Assuming that the intracluster gas is isothermal, its temperature  $T_{\text{gas}}$  is related to the total mass  $M$  by

$$k_B T_{\text{gas}}(M, z) = \gamma \frac{\mu m_p G M}{3 r_{\text{vir}}(M, z)}, \quad (7)$$

where  $k_B$  is the Boltzmann constant,  $G$  is the gravitational constant,  $m_p$  is the proton mass,  $\mu$  is the mean molecular weight (we adopt  $\mu = 0.59$ ), and  $\gamma$  is a fudge factor of order unity which may be calibrated from hydrodynamical simulations or observations. The virial radius  $r_{\text{vir}}(M, z_f)$  for objects formed at  $z_f$  is computed from the nonlinear spherical collapse model as

$$\begin{aligned} r_{\text{vir}}(M, z_f) &= 1.69(1+z_f) \left( \frac{\Delta_{\text{vir}}}{18\pi^2} \right)^{-1/3} \\ &\times \left( \frac{M}{10^{15} \Omega_0 h^2 M_\odot} \right)^{1/3} \text{ Mpc}, \end{aligned} \quad (8)$$

where  $\Delta_{\text{vir}}(\Omega_0, \lambda_0, z_f)$  denotes the density of objects virialized at  $z_f$  in units of the mean density of the universe at that epoch and is explicitly given in Kitayama & Suto (1996b). Assuming that  $z_f$  is the same as the observed redshift of clusters  $z$ , equation (7) is written as

$$T_{\text{gas}}(M, z) = 5.2\gamma(1+z) \left( \frac{\Delta_{\text{vir}}}{18\pi^2} \right)^{1/3} \times \left( \frac{M}{10^{15} M_{\odot}} \right)^{2/3} \Omega_0^{1/3} h^{2/3} \text{ keV}. \quad (9)$$

Finally, we compute the mass function  $n_M(M, z)dM$  in equation (1) using the Press-Schechter theory (Press & Schechter 1974) assuming  $z = z_f$  as above. The effect of  $z_f \neq z$  is discussed by KS97 in this context, and the more general consideration of  $z_f \neq z$  is given in Lacey & Cole (1993), Sasaki (1994), and Kitayama & Suto (1996a,b).

## 2.2. Submm flux from clusters due to the Sunyaev-Zel'dovich effect

The inverse-Compton scattering of the CMB photons due to high temperature electron gas leads to distortion of the CMB spectrum. Sunyaev & Zel'dovich (1972) showed that the specific intensity of the distorted CMB spectrum at angular position  $\vec{\theta}$  from the center of a cluster is written as

$$I_{\nu}(\vec{\theta}) = i_0(1+z)^3 x^3 f_{\text{BB}}(x) + \Delta I_{\nu}(\vec{\theta}), \quad (10)$$

$$\Delta I_{\nu}^{\text{NR}}(\vec{\theta}) = i_0(1+z)^3 g(x) y(\vec{\theta}), \quad (11)$$

$$g(x) = \frac{x^4 e^x}{(e^x - 1)^2} \left( x \coth \frac{x}{2} - 4 \right), \quad (12)$$

$$y(\vec{\theta}) = \int_{-\infty}^{\infty} \frac{k_B T_{\text{gas}}(z)}{m_e c^2} \sigma_T n_e(\vec{\theta}, l) dl, \quad (13)$$

where  $i_0 = 2(k_B T_{\text{CMB},0})^3 / (h_p c)^2$ ,  $x = h_p \nu(z) / (k_B T_{\text{CMB},z})$ ,  $f_{\text{BB}}(x) = 1/(e^x - 1)$ ,  $T_{\text{CMB},z} = (1+z)T_{\text{CMB},0}$  is the temperature of the CMB at  $z$  ( $T_{\text{CMB},0} = 2.726$  K),  $h_p$  is the Planck constant,  $\sigma_T$  is the Thomson cross section,  $m_e$  is the electron mass, and  $n_e$  is the electron number density in the cluster. All the quantities in the above equations are evaluated at the rest-frame of the cluster located at  $z$ , which explains the explicit  $(1+z)$  dependence. Note that  $x$  is simply written in terms of the observed frequency  $\nu_0$  as  $x = h_p \nu_0 / (k_B T_{\text{CMB},0})$ . At frequencies  $\nu_0 > 217\text{GHz}$  (or wavelengths  $\lambda_0 < 0.14\text{cm}$ ),  $g(x)$  becomes positive and galaxy clusters become positive sources. In what follows we consider mainly the submm band at the observed wavelength  $\lambda_0 = 0.85\text{mm}$  ( $\nu_0 = 350\text{GHz}$ ) where the emission from clusters is fairly strong ( $x = 6.2$  and  $g(x) = 6.7$ ) and the ground observations are feasible.

Then a total specific intensity from a cluster of galaxies at  $z$  is given by its volume integral:

$$I_{\nu}^{\text{NR}}(x, z) \equiv i_0(1+z)^3 g(x) \int \frac{k_B T_{\text{gas}}(z)}{m_e c^2} \sigma_T n_e dV. \quad (14)$$

So the cluster of mass  $M$  observed at  $z$  is equivalent to a source with the “typical” luminosity of  $L^{\text{NR}} \equiv 4\pi\nu I_\nu^{\text{NR}}(x, z)$  at submm bands, and equations (8) and (9) yield

$$L^{\text{NR}}(x, M, z) = 6.4 \times 10^{44} \Omega_B (1+z)^4 \left( \frac{x}{6.2} \right) \left[ \frac{g(x)}{6.7} \right] \frac{1+X}{2} \\ \times \left( \frac{\Delta_{\text{vir}}}{18\pi^2} \right)^{1/3} \left( \frac{M}{10^{15} M_\odot} \right)^{5/3} \left( \frac{h}{\Omega_0} \right)^{2/3} \text{ erg/s}, \quad (15)$$

where  $X$  is the hydrogen mass fraction and set to 0.76 in the analysis below,  $\nu(z) = (1+z)k_B x T_{\text{CMB},0}/h_p$ , and we adopt the baryon density parameter  $\Omega_B = 0.0125h^{-2}$ . Similarly we can write the averaged submm flux  $S_\nu^{\text{NR}}(x, M) \equiv I_\nu^{\text{NR}}(x)/d_L^2(z)$  of the cluster (Barbosa et al. 1996) as

$$S_\nu^{\text{NR}}(x, M) = 25 g(x) \frac{1+X}{2} \Omega_b \Omega_0^{-2/3} h^{8/3} \frac{1+z}{D_A^2(z)} \\ \times \left( \frac{\Delta_{\text{vir}}}{18\pi^2} \right)^{1/3} \left( \frac{M}{10^{15} M_\odot} \right)^{5/3} \text{ mJy}. \quad (16)$$

It should be noted that the above flux corresponds to the mean value over the entire cluster, and the observed  $\log N$ – $\log S$  might be somewhat different depending on the details of the instruments specifically used for the survey. Aghanim et al. (1997) address this issue in detail.

Relativistic correction to equation (11) becomes important for  $T_{\text{gas}} \gtrsim 10$  keV especially at submm bands. Rephaeli (1995; see also Rephaeli & Yankovitch 1997) obtained the following approximate expressions for the flux change:

$$\Delta I_\nu^{\text{R}}(\vec{\theta}) = i_0 x^3 f_{\text{BB}}(x) \eta y(\vec{\theta}) [\Phi_{\text{iso}}(x, \eta) - 1], \quad (17)$$

$$\eta = m_e c^2 / (k_B T_{\text{gas}}), \quad (18)$$

$$\Phi_{\text{iso}}(x, \eta) = B(\eta) \phi(x, \eta), \quad (19)$$

$$B(\eta) = \left[ 4 \int_0^1 \beta_e^2 \gamma_e^5 e^{-\eta \gamma_e + \eta} d\beta_e \right]^{-1}, \quad (20)$$

$$\phi(x, \eta) = \int_0^1 \left[ \frac{1}{e^{xt} - 1} + \frac{1}{t^3 (e^{x/t} - 1)} \right] \\ \times (e^x - 1) \zeta(t, \eta) dt, \quad (21)$$

$$\zeta(t, \eta) = \int_{(1-t)/(1+t)}^1 [(1 + \beta_e)t - 1 + \beta_e] \\ \times \gamma_e^3 e^{-\eta \gamma_e + \eta} d\beta_e, \quad (22)$$

where the integration is carried out over the electron velocity  $\beta_e$  in units of  $c$  and the fractional frequency shift  $t = \nu/\nu'$  of the photon from  $\nu$  to  $\nu'$  assuming that the scattering is isotropic in the electron rest frame, and  $\gamma_e = 1/\sqrt{1 - \beta_e^2}$ .

At  $\lambda = 0.85\text{mm}$ , we find that the above relativistic correction is well fitted by

$$\Delta I_\nu^{\text{R}} \equiv \left[ 1 - 0.012 \left( \frac{T_{\text{gas}}(z)}{1\text{keV}} \right) \right] \Delta I_\nu^{\text{NR}}. \quad (23)$$

While clusters with  $T_{\text{gas}} \gtrsim 10\text{keV}$  are rare and the above correction does not make significant difference, we take it into account for completeness in computing submm luminosity functions and the  $\log N$ – $\log S$ .

Since the above submm flux after the relativistic correction,  $S_\nu^{\text{R}}(x, M)$ , is explicitly expressed as a function of  $M$  and  $z$ , the submm  $\log N$ – $\log S$  is computed in a similar manner to equation (1):

$$N(> S_\nu) = \int_0^\infty dz d_A^2(z) c \left| \frac{dt}{dz} \right| \times \int_{S_\nu}^\infty dS_\nu^{\text{R}} (1+z)^3 n_M(M, z) \frac{dM}{dS_\nu^{\text{R}}}. \quad (24)$$

### 3. Number counts in X-ray and submm bands predicted in the cold dark matter models

KS97 shows that CDM models with a certain range of parameters reproduce the *ROSAT*  $\log N$ – $\log S$  data as well as the XTF (Henry & Arnaud 1991) and the *COBE* 4 year data (Bunn & White 1997). To be definite, we consider five models with different sets of parameters summarized in table 1, and see if one can break the degeneracy of the models by comparing the  $\log N$ – $\log S$  relations in different bands.

Figure 1 shows the  $\log N$ – $\log S$  of clusters of galaxies in the soft X-ray (0.5-2 keV) band (*left*), in the hard X-ray (2-10 keV) band (*middle*), and at the submm (0.85mm) band (*right*). Throughout this paper, we assume that the primordial spectral index  $n$  is equal to unity and use the fitting formulae given in Kitayama & Suto (1996b) for the CDM mass fluctuation spectrum on the basis of Bardeen et al. (1986) transfer function. The degeneracy in the 0.5-2 keV band  $\log N$ – $\log S$  is shown to be broken at the submm band, and at a lesser extent in the 2-10 keV band.

To see this more clearly, we plot in figure 2 the contour maps of the cluster  $\log N$ – $\log S$  in different bands on the  $\Omega_0 - \sigma_8$  plane. For the 0.5-2 keV band, the  $1 - \sigma$  significance level derived from the  $\chi^2$  test between our theoretical prediction and the observation is plotted, while for the 2-10 keV and submm bands, the contours of the number of clusters per steradian ( $1, 10, 10^2, 10^3, 10^4$  from bottom to top) at  $S(2\text{-}10 \text{ keV}) = 10^{-12} \text{ erg cm}^{-2} \text{ s}^{-1}$  and  $S_\nu(0.85\text{mm}) = 10^3 \text{ mJy}$  are plotted respectively. The  $\sigma_8$  values derived from the *COBE* 4 year data (Bunn & White 1997) is also shown for reference. The contours for the 2-10 keV band counts run almost parallel to the  $\chi^2$  contour of the 0.5-2 keV band counts. In this sense, the future *ASCA*  $\log N$ – $\log S$  data will provide an independent consistency check of the *ROSAT* data. The shape of the submm  $\log N$ – $\log S$  contours, on the other hand, is quite different, especially at high  $\sigma_8$ , and thus should place complementary constraints on  $\Omega_0$  and  $\sigma_8$ . In addition to the conventional CDM spectrum whose shape vary with  $\Omega_0$ ,  $h$  and  $\Omega_{\text{B}}$ , we adopt here the ‘CDM-like’ power spectrum with the fixed shape parameter  $\Gamma = 0.25$  (lower panels in fig. 2). The corresponding  $\log N$ – $\log S$  contours are similar to the CDM case except at  $\Omega_0 \lesssim 0.2$  and  $\Omega_0 \gtrsim 0.8$ , while the *COBE* normalized  $\sigma_8$  is

very sensitive to the changes in the spectral shape.

#### 4. Evolution of cluster abundances

The evolutionary behavior of the cluster abundance would provide a useful probe of the cosmological parameters as discussed by a number of authors (e.g., Viana & Liddle 1996; Eke, Cole, Frenk 1996; Oukbir & Blanchard 1997; Mathiesen & Evrard 1997). It is of particular importance because the current and near future observations will provide us with the rapidly increasing amount of information on high redshift clusters. Thus we consider the evolution of cluster distribution and discuss whether one can break the degeneracy among the models inferred from the soft X-ray  $\log N$ – $\log S$  relation (table 1).

Figure 3 exhibits the cumulative distribution of clusters against  $z$  in different bands. As expected, the evolutionary behavior strongly depends on the value of  $\Omega_0$ ; the fraction of low redshift clusters becomes larger for greater  $\Omega_0$ . In the 0.5-2 keV band, where the cumulative number of clusters over whole redshift range is by definition the same for all models, the numbers at  $z < 0.2$  are quite different among the models. This suggests that one may be able to distinguish these models merely by determining the redshifts of clusters at  $z \lesssim 0.2$  (see also discussion below).

In order to characterize the physical properties of galaxy clusters, we have so far focused on their flux, because it is the simplest quantity which can be determined primarily from observations. Another major quantity of clusters is their temperature. Although the sample of clusters with measured temperature is still limited, an increasing amount of temperature information is going to become available from the *ASCA* (and future) observations. Furthermore, the temperature has an advantage in that it is insensitive to the detailed distribution of intracluster gas and much easier to model, compared to the X-ray flux or luminosity. This is in fact the main reason why many of the previous analysis of cluster abundance and its evolution are based upon the temperature rather than the X-ray luminosity (White, Efstathiou & Frenk 1993; Viana & Liddle 1996; Eke et al. 1996). However, the observed samples of clusters are usually flux limited, which needs to be kept in mind when one compares the theoretical predictions with the observed statistics. In our present framework, it is possible to incorporate explicitly the effects of limiting fluxes in the analysis based upon the cluster temperature.

Figures 4 and 5 show the cumulative distribution of clusters with temperature greater than  $T$ , redshift less than  $z$ , and with/without the X-ray flux limit. It is apparent that the presence of a flux limit affects significantly the temperature distribution and its evolution. For the flux limit of  $S = 10^{-12}$  erg cm $^{-2}$  s $^{-1}$  in the 0.5-2 keV band, the number of clusters  $N(> S, > T, < z)$  per unit solid angle with  $T = 1$  keV is reduced by an order of magnitude at  $z = 0.1$  and by over three orders of magnitude at  $z = 1$ , while the number of those with  $T = 5$  keV is less affected.

The above discussion has clarified that the redshift evolution (at low  $z$ ) and the temperature distribution of a given cluster sample with a specific flux limit can provide a useful probe of



cosmological models. Unfortunately, we do not yet have a complete X-ray cluster sample with redshift and temperature information. However, one may still demonstrate the power of this approach using currently available 'best' sample. For this purpose, we tentatively adopt the X-ray brightest Abell-type clusters (XBACs, Ebeling et al. 1996), which is about 80 % complete and consists of 242 clusters with  $S > 5 \times 10^{-12}$  erg cm $^{-2}$  s $^{-1}$  in the 0.1-2.4 keV band and  $z < 0.2$ . We use the temperature and redshift data compiled in table 3 of Ebeling et al. (1996). About 92 % and 30 % of all the clusters listed in this table have measured redshift and temperature, respectively. For the rest of the sample, the table also provides the redshifts estimated from the magnitude of the 10th-ranked cluster galaxy, and the temperatures estimated from the empirical  $L - T$  relation. Keeping in mind the incompleteness of the sample and uncertainties especially in the estimated temperature data, we simply intend to perform a crude comparison with our predictions.

The results are plotted in figures 6, 7 and 8. The sky coverage of the XBACs is hard to quantify mainly due to the uncertain volume incompleteness of the underlying optical catalogue as notified by Ebeling et al. (1996). In these figures, therefore, we simply plot the real numbers of the XBACs and normalize our model predictions to match the total number of the XBACs at the flux limit  $S(0.1-2.4 \text{ keV}) = 5 \times 10^{-12}$  erg cm $^{-2}$  s $^{-1}$  and redshift  $z = 0.2$  (Fig. 6). In general, the model predictions are shown to be capable of reproducing well the shape and amplitude of the observed distributions  $N(> S, > T, < z)$  even when  $T$  and  $z$  are varied (Figs 7 and 8). Taking into account the incompleteness of the observed data and large statistical fluctuations at low numbers, the agreements with models L03 and L03 $\gamma$  (both has  $\Omega_0 = 0.3$ ) are rather remarkable. Since the shapes and amplitudes of the predicted curves in these figures are primarily determined by the value of  $\Omega_0$ , this result provides a further indication for low  $\Omega_0$  universe.

## 5. Contribution to the X-ray and submm background radiation

The currently observed X-ray log $N$ -log $S$  especially at faint flux end (Rosati et al. 1997; Rosati & Della Ceca 1997) places a model-independent constraint on the cluster contribution to the soft XRB. To see this, let us note that the observed log $N$ -log $S$  in the 0.5-2 keV band plotted in figure 1 is roughly fitted by

$$\begin{aligned} N(> S) &\sim 200(S/S_{12})^{-1} \text{ str}^{-1} (S \lesssim S_{12}), \\ &\sim 200(S/S_{12})^{-1.3} \text{ str}^{-1} (S \gtrsim S_{12}), \end{aligned} \quad (25)$$

where we define  $S_{12} \equiv 10^{-12}$  erg cm $^{-2}$  s $^{-1}$ . The above relation implies that the cluster contribution to the XRB is

$$\begin{aligned} I^{\text{cl}}(0.5-2 \text{ keV}) &= \int_{S_{\min}}^{\infty} S \left| \frac{dN}{dS} \right| dS \\ &\sim 2 \times 10^{-10} \left( \ln \frac{S_{12}}{S_{\min}} + 4.3 \right) \text{ erg cm}^{-2} \text{ s}^{-1} \text{ str}^{-1}. \end{aligned} \quad (26)$$

Although the only uncertain parameter in the above estimate is the faint end flux  $S_{\min}$ , its dependence is very weak. If we take  $S_{\min} = 10^{-15}$  erg cm $^{-2}$  s $^{-1}$ , for instance,  $I_{\text{cl}}(0.5\text{-}2 \text{ keV}) \sim 2 \times 10^{-9}$  erg cm $^{-2}$  s $^{-1}$ str $^{-1}$ , which is less than 10 % of the observed XRB (Gendreau et al. 1995; Suto et al. 1996).

To be more specific, we also compute numerically the contribution of clusters to the XRB. The XRB intensity  $I_{\nu}^{\text{cl}}(E_0)$  from clusters at energy  $E_0$ , as seen by an observer at present, is given by

$$I_{\nu}^{\text{cl}}(E_0) = \frac{c}{4\pi H_0} \int_0^{\infty} dz \times \frac{J_{\nu}[E_0(1+z), z]}{(1+z)\sqrt{\Omega_0(1+z)^3 - K(1+z)^2 + \lambda_0}}, \quad (27)$$

where  $J_{\nu}(E, z)$  is the comoving space-averaged volume emissivity at redshift  $z$ . We estimate this quantity by

$$J_{\nu}(E, z) = \int_0^{\infty} L_{\nu}(E, M, z) n_M(M, z) dM, \quad (28)$$

where the luminosity  $L_{\nu}(E, M, z)$  of a cluster of mass  $M$  at  $z$  is computed in a similar manner to Section 2.1. It should be noted that the observed XRB spectrum is not derived from all sky surveys (in particular, at lower energy band), but from small regions in the sky where there are very few known bright X-ray sources. In order to compare with such observations, therefore, we also need to omit bright sources in our theoretical predictions by equation (27). For this purpose, we only consider contributions from clusters with flux below the critical value:

$$S_{\text{crit}}(0.5\text{-}2 \text{ keV}) = 10^{-13} \text{ erg cm}^{-2} \text{ s}^{-1}, \quad (29)$$

which roughly corresponds to the flux of the brightest X-ray source observed in the Lockman Hole by *ROSAT* (Hasinger et al. 1993).

Figure 9 exhibits the XRB intensity from clusters of galaxies in the cases of models L03 and E1, both of which reproduce the observed  $\log N$ – $\log S$  relation in the soft X-ray (0.5-2 keV) band. In these models, clusters contribute to the XRB only less than 20 % at  $E_0 \lesssim 2\text{keV}$ , which is consistent with the rough estimate described above. Thus, clusters of galaxies cannot be the major sources for the XRB even in soft X-ray bands (Evrard & Henry 1991; Oukbir, Bartlett, Blanchard 1997). As is clear from the above analysis, this conclusion is based on the observed  $\log N$ – $\log S$  relation, and almost independent of the assumed cosmological parameters. In fact, if one adopts a theoretical  $L_{\text{bol}} - T$  relation inferred from the self-similar assumption (Kaiser 1986) which yields  $\alpha = 2$  in equation (5), there exist some models in which clusters account for the entire soft XRB (Blanchard et al. 1992; Kitayama & Suto 1996a). Such models, however, are simply in conflict with both the observed  $L_{\text{bol}} - T$  relation ( $\alpha = 3 \sim 3.5$ ) and the *ROSAT*  $\log N$ – $\log S$ .

A similar analysis can be performed for the SBR. Since we do not yet have the observed  $\log N$ – $\log S$  in the submm band, we fit the predicted  $\log N$ – $\log S$  of model L03 as follows:

$$N(> S_{\nu}) \sim 10^3 (S_{\nu}/100\text{mJy})^{-1.5} \text{ str}^{-1}, \quad (30)$$

at  $\lambda = 0.85\text{mm}$  ( $\nu = 350\text{GHz}$ ). Then we repeat the similar evaluation to equation (26) and obtain

$$\nu I_{\nu}^{\text{cl}}(0.85\text{mm}) \sim 10^{-12} \left( \frac{S_{\nu,\text{min}}}{100\text{mJy}} \right)^{-0.5} \text{W m}^{-2} \text{str}^{-1}. \quad (31)$$

Taking  $S_{\nu,\text{min}} = 1\text{mJy}$  gives  $\nu I_{\nu}^{\text{cl}}(0.85\text{mm}) \sim 10^{-11} \text{W m}^{-2} \text{str}^{-1}$ , which is only 3% of the value given in Puget et al. (1996):

$$\nu I_{\nu} \sim 3.4 \times 10^{-9} (\lambda/0.4\text{mm})^{-3} \text{W m}^{-2} \text{str}^{-1}, \quad (32)$$

in the 0.1 – 1 mm range. Results from the numerical integration shown in figure 10 confirm that the clusters of galaxies do not make a significant contribution to the SBR.

## 6. Conclusions

We have presented several cosmological implications of the number counts of clusters of galaxies. We have paid particular attention to the theoretical models which are in good agreement with the *ROSAT*  $\log N$ – $\log S$  in the soft X-ray band, and explored possibilities to further constrain the models from future observations in the *ASCA* hard X-ray and submm bands.

In the submm band ( $\lambda = 0.85\text{mm}$ ), models which reproduce the *ROSAT*  $\log N$ – $\log S$  predict  $N(> S_{\nu}) \sim (10^2 - 10^4)(S_{\nu}/100\text{mJy})^{-1.5} \text{str}^{-1}$  at  $S_{\nu} \gtrsim 100\text{mJy}$ . We have shown that the amplitude of the above relation depend sensitively on  $\Omega_0$  and  $\sigma_8$ , and in a substantially different manner from the *ROSAT*  $\log N$ – $\log S$ . Thus, combining the two can break the degeneracy in the acceptable parameter region on the  $\Omega_0 - \sigma_8$  plane. This indicates that the future observations by the European *PLANCK* mission and the Japanese *LMSA* project would provide powerful probes of these parameters. The number counts in the *ASCA* 2-10 keV band, show similar parameter dependence to those in the *ROSAT* 0.5-2 keV band, and we predict  $N(> S) \sim 200(S/10^{-12}\text{erg cm}^{-2} \text{s}^{-1})^{-1.3} \text{str}^{-1}$  at  $S \gtrsim 10^{-12}\text{erg cm}^{-2} \text{s}^{-1}$  in the *ASCA* 2-10 keV band. Therefore the *ASCA*  $\log N$ – $\log S$  would provide an important cross-check for our interpretation of the *ROSAT*  $\log N$ – $\log S$  data.

The evolutionary behavior of the number counts are also important to put additional cosmological constraints. We have exhibited that, given a complete flux limited cluster sample with redshift and/or temperature information, one can further constrain the cosmological models. We have performed a tentative comparison between our theoretical predictions and the recent compilation of the XBACs by Ebeling et al. (1996), which is the largest sample of galaxy clusters available to date. While the incompleteness of the sample and uncertainties in the temperature data still make it difficult to draw any definite conclusions from this comparison, it is interesting to note that our predictions reproduce well the evolutionary features of the XBACs and that the results, although preliminary, seem to favor low density ( $\Omega_0 \sim 0.3$ ) universes.

The cluster  $\log N$ – $\log S$  also provides a tight constraint on their contribution to the background radiation in the corresponding energy band. Based on the  $\log N$ – $\log S$  relation observed by *ROSAT*

in the 0.5-2 keV band, we conclude that clusters of galaxies contribute at most 20% of the total X-ray and submm background radiations.

We deeply thank Piero Rosati and Harald Ebeling for generously providing us with the X-ray data prior to their publication, and Kuniaki Masai for helpful discussion and kindly making his code to compute the X-ray spectrum available to us. We are grateful to Alain Blanchard for calling our attention to his earlier work on the X-ray and submm number counts of galaxy clusters, and Yoel Rephaeli for useful correspondences on the relativistic correction of the SZ effect. T.K. acknowledges support from a JSPS (Japan Society of Promotion of Science) fellowship (09-7408). This research was supported in part by the Grants-in-Aid for the Center-of-Excellence (COE) Research of the Ministry of Education, Science, Sports and Culture of Japan (07CE2002) to RESCEU (Research Center for the Early Universe).

### References

- Aghanim, A., De Luca, A., Bouchet, F.R., Gispert, R., Puget, J.L. 1997, astro-ph/9705092  
Barber, C.R. et al. 1996, MNRAS 282, 157  
Barbosa, D., Bartlett, J.G., Blanchard, A., Oukbir, J. 1996, A&A 314, 13  
Bardeen, J. M., Bond, J. R., Kaiser, N., Szalay, A. 1986, ApJ 304, 15  
Blanchard, A., Wachter, K., Evrard, A.E., Silk, J. 1992, ApJ 391, 1  
Bower, R. G. 1997, astro-ph/9701014  
Bunn, E. F., White, M. 1997, ApJ 480, 6  
Colafrancesco, S., Mazzotta, P., Rephaeli, Y., Vittorio, N. 1997, ApJ 479, 1  
David, L. P., Slyz, A., Jones, C., Forman, W., Vrtilek, S. D. 1993, ApJ 412, 479  
Ebeling, H., Voges, W., Böhringer, H., Edge, A. C., Huchra, J. P., Briel, U. G. 1996, MNRAS 281, 799  
Ebeling, H., Edge, A. C., Fabian, A.C., Allen, S. W., Crawford C. S. 1997a, ApJ 479, L101  
Ebeling H., et al. 1997b, MNRAS submitted  
Eke, V. R., Cole, S., Frenk, C. S. 1996, MNRAS 282, 263  
Evrard, A.E., Henry, J. P. 1991, ApJ 383, 95  
Gendreau, K.C. et al. 1995, PASJ 47, L5  
Hasinger, G. 1992, in The X-ray Background, eds. Barcons, X., Fabian, A. C. (Cambridge U.P.: Cambridge), 229  
Hasinger, G., Burg, R., Giacconi, R., Hartner, G., Schmidt, M., Trümper, J., Zamorani, G. 1993, A&A 275, 1  
Henry, J. P., Arnaud, K. A. 1991, ApJ 372, 410  
Kaiser N. 1986, MNRAS 222, 323  
Kaiser N. 1991, ApJ 383, 104  
Kitayama, T., Suto, Y. 1996a, MNRAS 280, 638

- Kitayama, T., Suto, Y. 1996b, ApJ 469, 480  
 Kitayama, T., Suto, Y. 1997, ApJ 490, in press (KS97)  
 Lacey, C. G., Cole, S. 1993, MNRAS 262, 627  
 Masai, K. 1984, Ap&SS 98, 367  
 Mathiesen, B., Evrard, A. E. 1997, astro-ph/9703176  
 Mushotzky, R.F., Scharf, C. A. 1997, ApJ 482, L13  
 Oukbir, J., Blanchard, A. 1997, A&A 317, 10  
 Oukbir, J., Bartlett, J. G., Blanchard, A. 1997, A&A 320, 3650  
 Ponman, T. J., Bournier, P. D. J., Ebeling, H., Böhringer, H. 1996, MNRAS 283, 690  
 Press, W. H., Schechter, P. 1974, ApJ 187, 425 (PS)  
 Puget, J.-L., Abergel, A., Bernard, J.-P., Boulanger, F., Burton, W. B., Désert, F.-X., Hartmann, D. 1996, A&A 308, L5  
 Rephaeli Y. 1995, ARA&A 33, 541  
 Rephaeli Y., Yankovitch, D. 1997, ApJ 481, L55  
 Rosati, P., Della Ceca, R., Burg R., Norman, C., Giacconi, R. 1995, ApJ 445, L11  
 Rosati, P., Della Ceca, R. 1997, in preparation  
 Rosati, P., Della Ceca, R., Norman, C., Giacconi, R. 1997, ApJL submitted  
 Sasaki, S. 1994, PASJ 46, 427  
 Suto, Y., Makishima, K., Ishisaki, Y., Ogasaka, Y. 1996, ApJ 461, L33  
 Sunyaev R.A., Zel’dovich Ya.B. 1972, Commnts. Astrophys. Space Phys. 4, 173  
 Viana, P. T. P., Liddle, A. R. 1996, MNRAS 281, 323  
 White, S. D. M., Efstathiou, G., Frenk, C. S. 1993, MNRAS 262, 1023

Table 1. CDM model parameters from the *ROSAT* X-ray  $\log N$ – $\log S$  .

Model	$\Omega_0$	$\lambda_0$	$h$	$\sigma_8$	$\alpha$	$\gamma$
L03	0.3	0.7	0.7	1.04	3.4	1.2
O045	0.45	0	0.7	0.83	3.4	1.2
E1	1.0	0	0.5	0.56	3.4	1.2
L03 $\gamma$	0.3	0.7	0.7	0.90	3.4	1.5
L01 $\alpha$	0.1	0.9	0.7	1.47	2.7	1.2

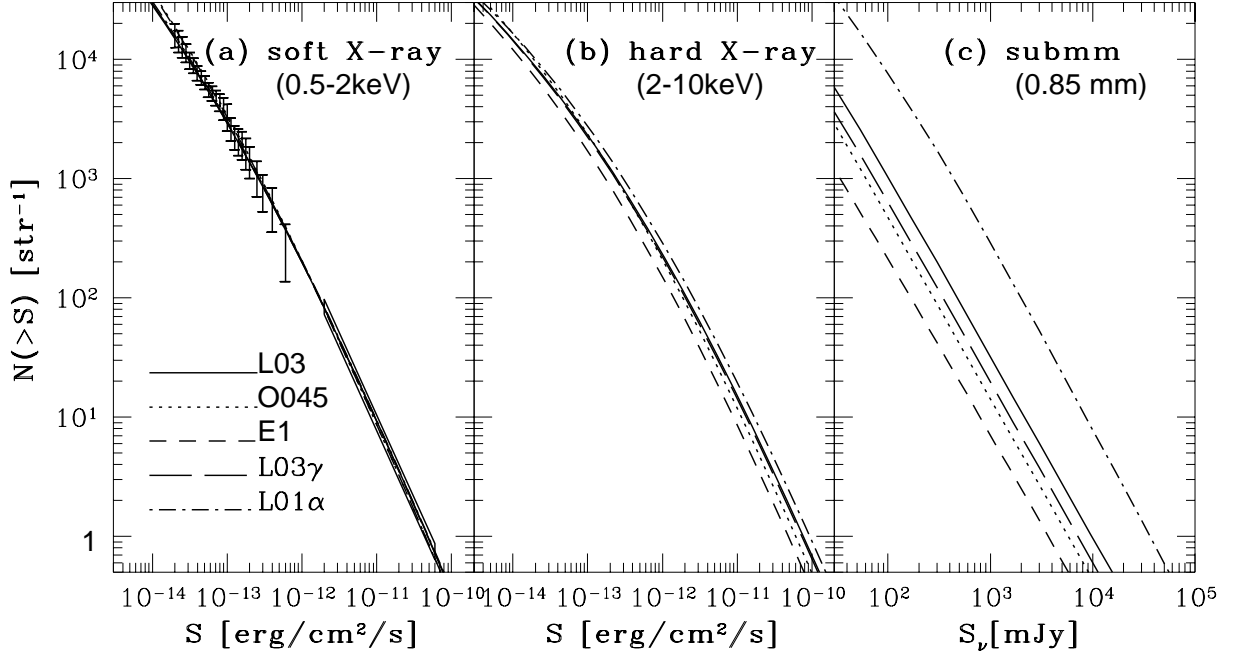


Fig. 1.— The  $\log N$ – $\log S$  relations of galaxy clusters for CDM models in (a) the soft X-ray (0.5–2.0 keV) band, (b) the hard X-ray (2–10 keV) band, and (c) the submm (0.85 mm) band. Also shown in panel (a) are the observed data with the error bars from the *ROSAT* Deep Cluster Survey (RDCS, Rosati et al. 1995, 1997), and the error box from the *ROSAT* Brightest Cluster Sample (BCS, Ebeling et al. 1997a,b). Lines represent the models listed in table 1; L03 (solid), O045 (dotted), E1 (short dashed), L03 $\gamma$  (long dashed), and L01 $\alpha$  (dot-dashed).

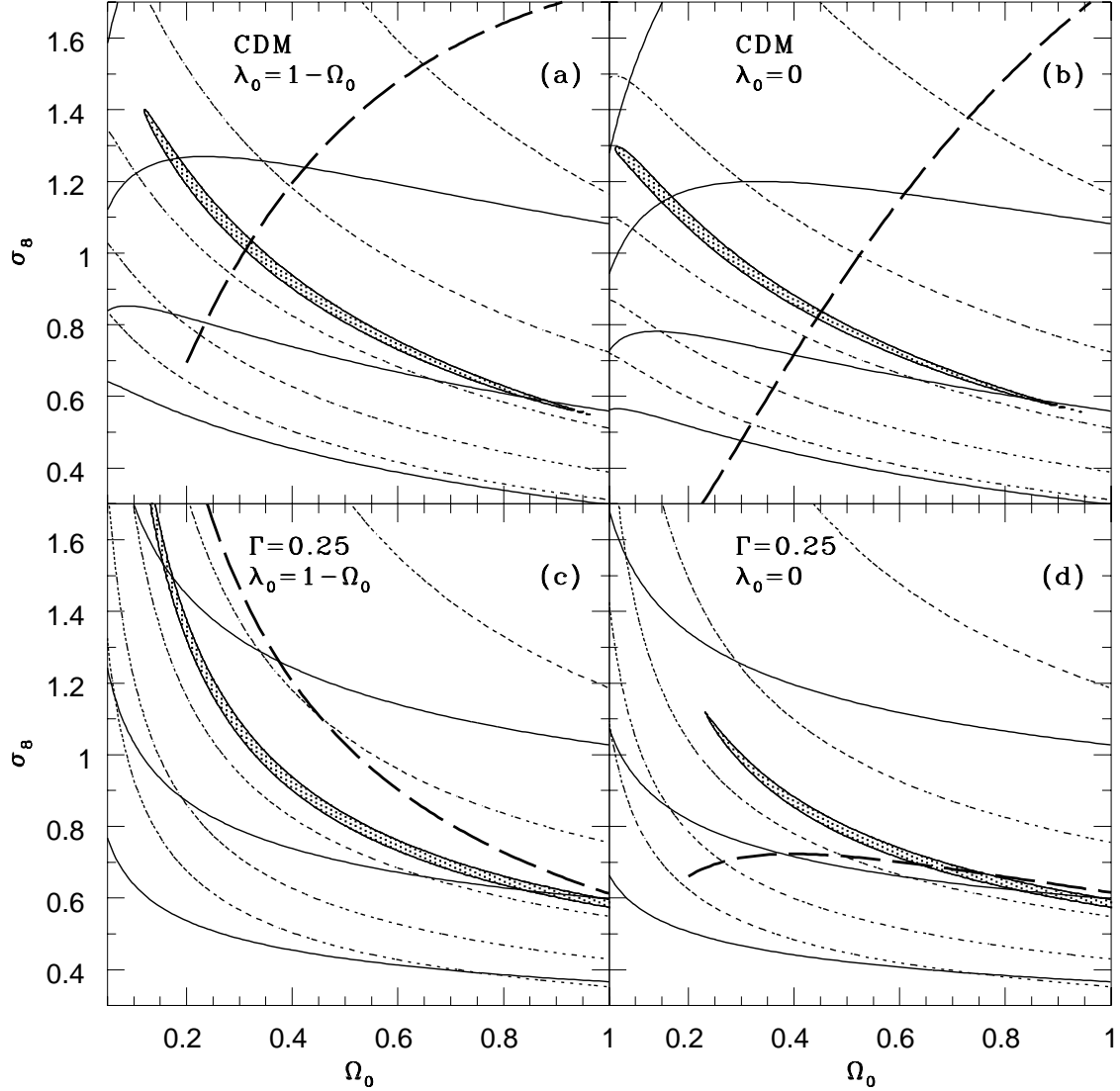


Fig. 2.— Contour maps on the  $\Omega_0$ - $\sigma_8$  plane in (a) spatially flat ( $\lambda_0 = 1 - \Omega_0$ ) CDM models, (b) open ( $\lambda = 0$ ) CDM models, (c) spatially flat CDM-like models with the fixed shape parameter ( $\Gamma = 0.25$ ), and (d) open CDM-like models with  $\Gamma = 0.25$ . In all cases,  $h = 0.7$ ,  $\alpha = 3.4$ , and  $\gamma = 1.2$  are assumed. Shaded regions represent the  $1 - \sigma$  significance contour derived in KS97 from the  $\chi^2$  test between our theoretical prediction and the observation in the soft X-ray (0.5-2 keV) band. Solid and dotted lines indicate the contours of the number of clusters greater than  $S$  per steradian (1, 10,  $10^2$ ,  $10^3$ ,  $10^4$  from bottom to top) with  $S = 10^{-12}$  erg cm $^{-2}$  s $^{-1}$  in the hard (2-10 keV) X-ray band and with  $S_\nu = 10^3$  mJy in the submm (0.85 mm) band, respectively. Thick dashed lines represent the *COBE* 4 year result computed from the fitting formulae at  $0.2 < \Omega_0 \leq 1$  by Bunn & White (1997).

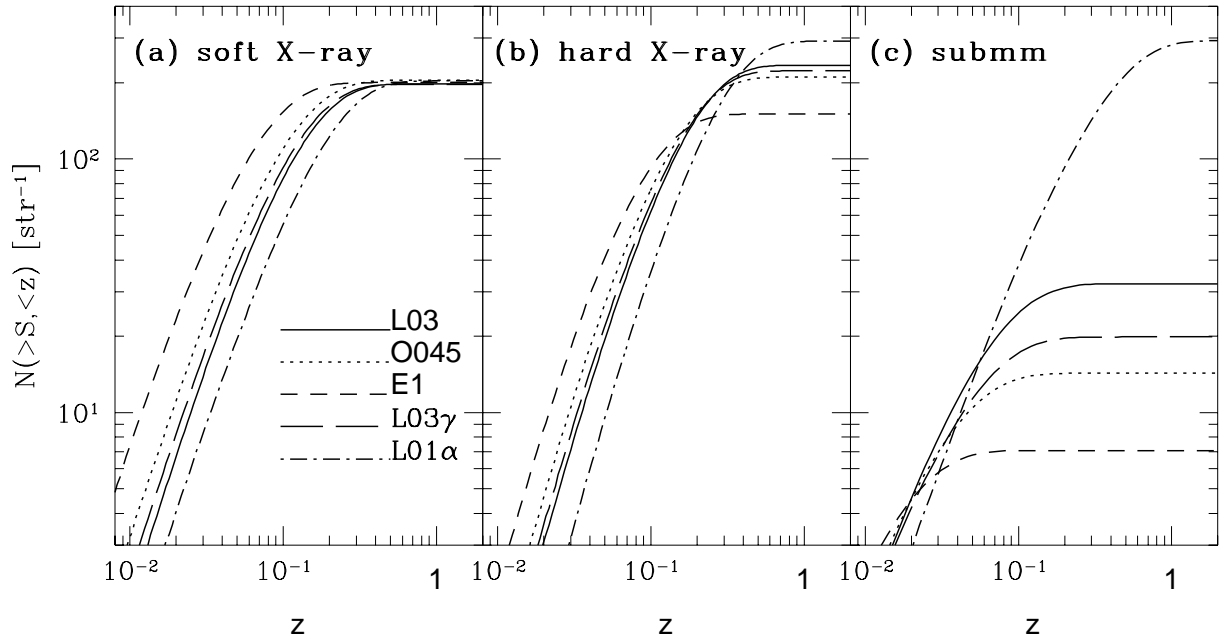


Fig. 3.— Cumulative distribution of galaxy clusters with flux greater than  $S$  and redshift less than  $z$ , as a function of  $z$  in (a) the soft X-ray (0.5-2 keV) band with  $S = 10^{-12} \text{ erg cm}^{-2} \text{ s}^{-1}$ , (b) the hard X-ray (2-10 keV) band with  $S = 10^{-12} \text{ erg cm}^{-2} \text{ s}^{-1}$ , and (c) the submm (0.85 mm) band with  $S_\nu = 10^3 \text{ mJy}$ .



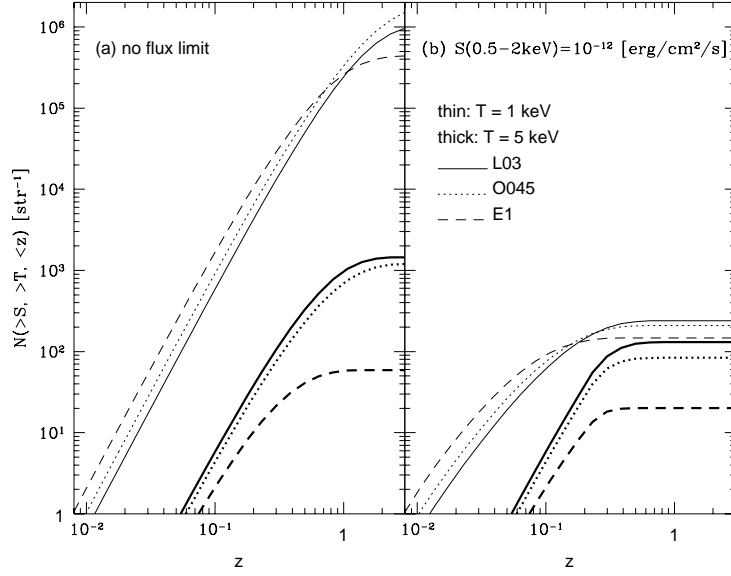


Fig. 4.— Cumulative distribution of galaxy clusters with flux greater than  $S$ , temperature greater than  $T$  and redshift less than  $z$ , as a function of  $z$ ; (a)  $S = 0$  (no flux limit), and (b)  $S = 10^{-12} \text{ erg cm}^{-2} \text{ s}^{-1}$  in the 0.5-2 keV band. Thin lines indicate  $T = 1\text{keV}$ , while thick lines  $T = 5\text{keV}$ .

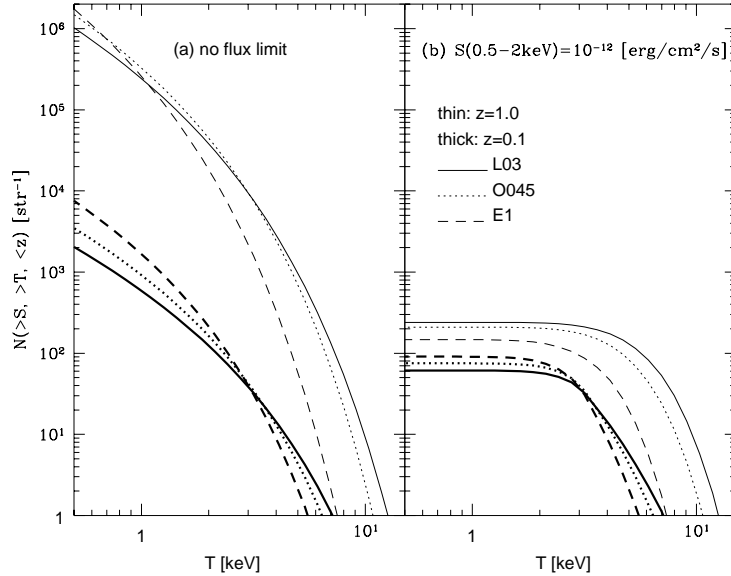


Fig. 5.— Same as Fig. 4, except that the distribution is plotted against  $T$  with thin lines indicating  $z = 1$  and thick lines  $z = 0.1$ .

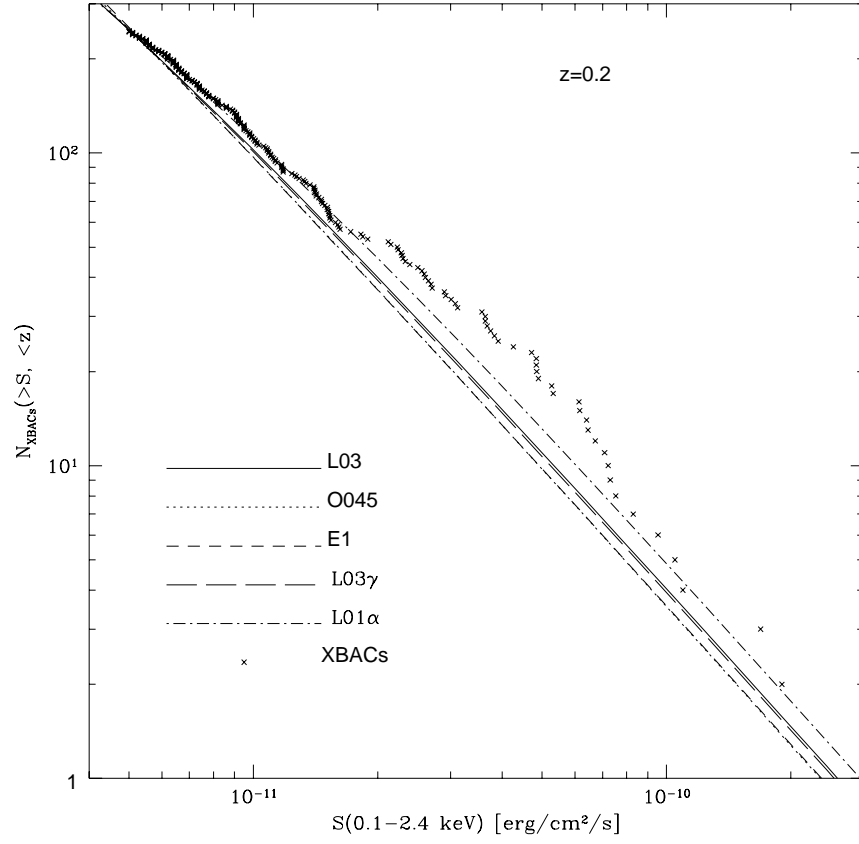


Fig. 6.— Tentative comparison with the XBACs (Ebeling et al. 1996) for the cumulative distribution  $N(> S, < z)$  with  $z=0.2$  against  $S$  in the 0.1-2.4 keV band. The model predictions are normalized to match the distribution of the XBACs at its flux limit of  $S(0.1-2.4 \text{ keV}) = 5 \times 10^{-12} \text{ erg cm}^{-2} \text{ s}^{-1}$ .

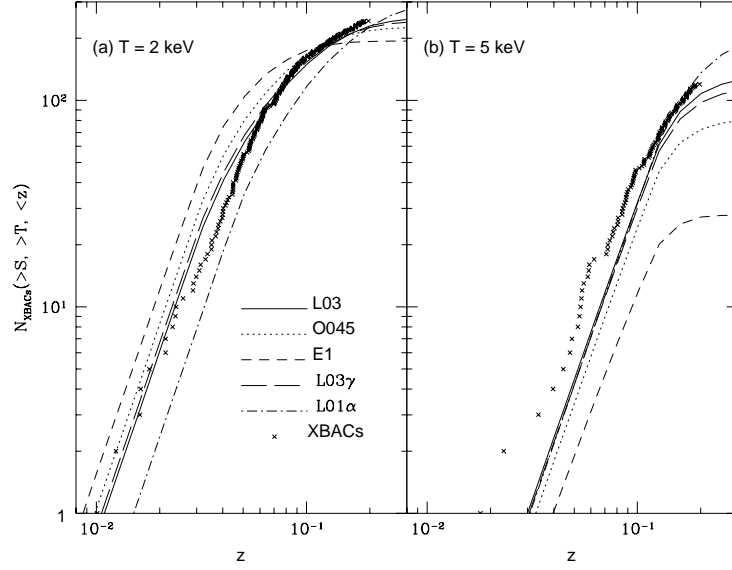


Fig. 7.— Same as Fig. 6, except that the distribution  $N(> S, > T, < z)$  is plotted against  $z$ , with (a)  $T = 1 \text{ keV}$ , and (b)  $T = 5 \text{ keV}$ . The flux limit is that of the XBACs,  $S(0.1\text{--}2.4 \text{ keV}) = 5 \times 10^{-12} \text{ erg cm}^{-2} \text{ s}^{-1}$ .

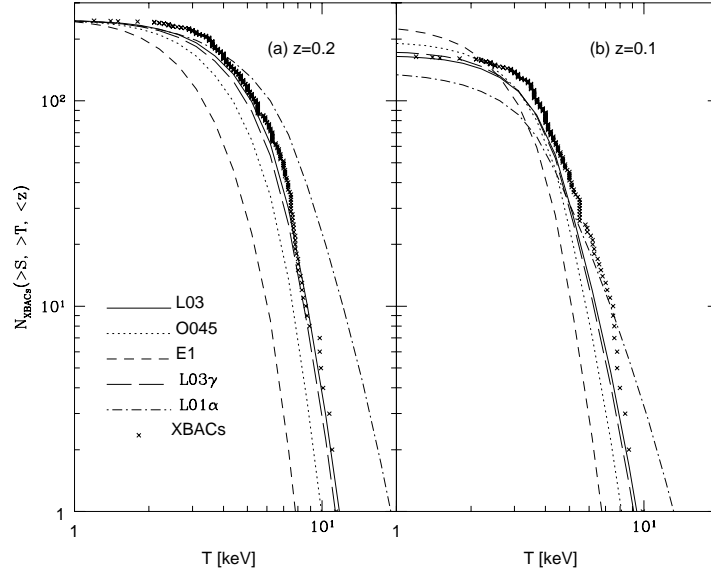


Fig. 8.— Same as Figs 6 and 7, except that the distribution  $N(> S, > T, < z)$  is plotted against  $T$  with (a)  $z = 0.2$ , and (b)  $z = 0.1$ . The flux limit is that of the XBACs,  $S(0.1\text{--}2.4 \text{ keV}) = 5 \times 10^{-12} \text{ erg cm}^{-2} \text{ s}^{-1}$ .

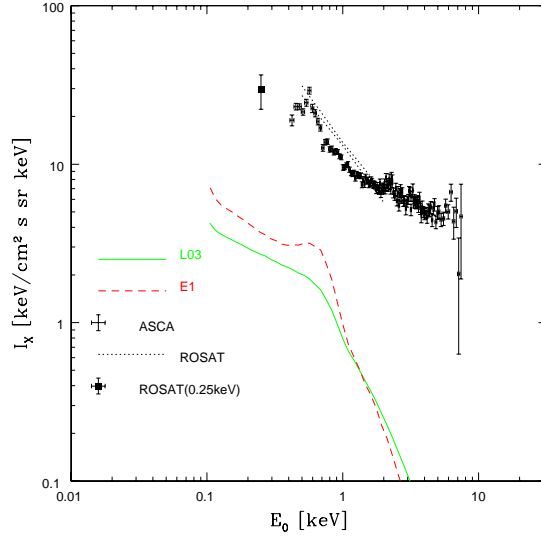


Fig. 9.— Contribution of clusters of galaxies to the XRB in models L03 (solid) and E1 (dashed). Also shown are the observed data: *ROSAT* 0.25 keV (Barber et al. 1996), *ROSAT* (Hasinger 1992), and *ASCA* (Gendreau et al. 1995).

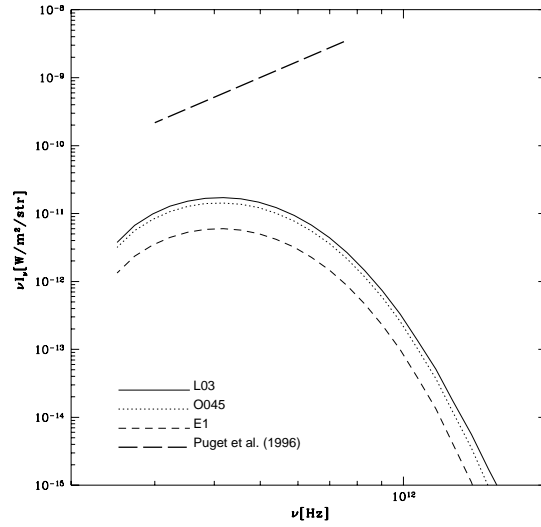


Fig. 10.— Contribution of clusters of galaxies to the SBR in models L03 (solid), O045 (dotted) and E1 (dashed). Also shown is the observed cosmic far-infrared background (Puget et al. 1996, thick dashed)